

A Lagrangian FEM Model to Produce Saw-toothed Macro-chip and to Study the Depth of Cut Influence on its Formation in Orthogonal Cutting of Ti6Al4V

F. Ducobu^a, E. Rivière-Lorphèvre^b and E. Filippi^c

University of Mons (UMONS), FPMs, Machine Design and Production Department,
20 Place du Parc, 7000 Mons, Belgium

^aFrancois.Ducobu@umons.ac.be, ^bEdouard.Riviere@umons.ac.be,
^cEnrico.Filippi@umons.ac.be

Keywords: Lagrangian, Ti6Al4V, chip formation, minimum chip thickness, size effect, saw-toothed chip, elastic spring back.

Abstract. The foundations of micro-milling are similar to macro-milling but the phenomena it involves are not a simple scaling-down of macro-cutting. The importance of the minimum chip thickness is one of the significant differences between the two processes. The lagrangian FEM model presented in this paper aims to study the depth of cut influence on chip formation of Ti6Al4V in orthogonal cutting. It is firstly used to compare the modelled saw-toothed macro-chip morphology and cutting forces to experimental cutting results from literature. Then a minimum chip thickness prediction is performed by decreasing the depth of cut. Finally this study is the opportunity to highlight the specific features of micro-cutting reported in literature, such as the effective negative rake angle of the tool or the size effect. The model presented brings therefore a numerical contribution to the comprehension of these phenomena.

Introduction

Due to the current miniaturization context the production of parts and features ranging from several mm to several μm is becoming a requirement. Micro-milling is one of the most flexible and fastest way to produce complex tridimensional micro-forms including sharp edges with a good surface finish in many materials (metallic alloys, composites, polymers and ceramics) [1, 2]. The material removal is performed by a miniature cutting tool (typical diameter between 100 μm and 500 μm) rotating at high speed. Its applications are found in many fields: micro-injection moulds, watch components, optical devices, components for the aerospace, biomedical and electronic industries are some of them.

Although the concepts of micro- and macro-milling are similar the scaling-down of the process induces some changes in the chip formation. Therefore the micro-cutting phenomenon cannot be considered as a simple scaling of macro-cutting.

The main difference between the two processes is the so-called ‘minimum chip thickness’ phenomenon, below which no chip is formed [1]. It can be observed when the ratio of the depth of cut on the tool edge radius (h/r) is smaller than the unit, as shown on Fig. 1, which is a common situation in micro-milling. It implies changes in the chip formation process.

One of the present challenges in micro-milling is the estimation of the minimum chip thickness value. This value greatly influences the chip formation and must be determined in order to correctly choose the cutting parameters. However this estimation is quite difficult because the minimum chip thickness depends on many parameters including the machined material and the tool geometry.

Two other specificities are observed in micro-cutting. Firstly, as the dimensions decrease the microstructure of the machined material becomes of the same order of magnitude as the tool edge radius and its granular structure must be taken into account [3]. Secondly, a nonlinear increase in the specific cutting energy is highlighted when the depth of cut decreases. This phenomenon observed in micro-cutting is known as the ‘size effect’ [4].

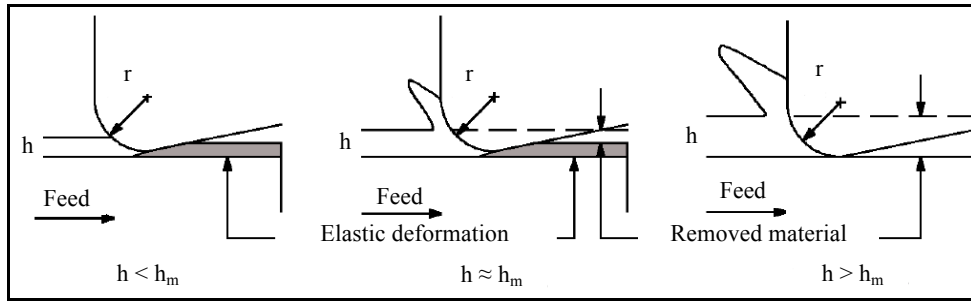


Fig. 1: Schematic representation of the minimum chip thickness phenomenon, inspired from [1] (r : edge radius, h : depth of cut, h_m : minimum chip thickness).

A numerical model suitable for micro-cutting could be interesting for investigation and modelling of these changes in the chip formation mechanism, but also to predict optimum cutting conditions (including the minimum chip thickness value).

This paper presents a first, simplified, proposition of such a numerical model.

Characteristics of the numerical model

The study of the depth of cut influence on chip formation in orthogonal cutting is performed through a Lagrangian Finite Element Method (FEM) model. It was developed with the commercial software ABAQUS/Explicit v6.8.

An important characteristic of this model is its validity in micro-cutting but also in macro-cutting. This allows to study changes in the cutting mechanism from macro- to micro-cutting with one single model. The ability to form saw-toothed chips in macro-cutting is one of the requirements (and difficulties) introduced by the multi-scale aspect of the model.

This 2D plane strain orthogonal cutting model focuses on the area where the chip is formed (close to the cutting edge of the tool). The cutting tool is modelled with a finite edge radius of $20\ \mu\text{m}$ in order to take into account its influence on chip formation. Its rake and clearance angles are set, respectively, to 15° and 2° . Fig. 2 presents the initial geometry and boundary conditions of the model. The cutting speed, V_c , is equal to $75\ \text{m/min}$. Three- and four-node linear elements are used to mesh the two parts. To give a rough idea of the mesh, the workpiece is made of around 18 000 elements and the tool of about 400 for the macro-cutting case.

The tool material is tungsten carbide and its behaviour is described by a linear elastic law. The workpiece material is Ti6Al4V. The model does not take the granular structure of Ti6Al4V into account and constitutes therefore a simplification of micro-cutting.

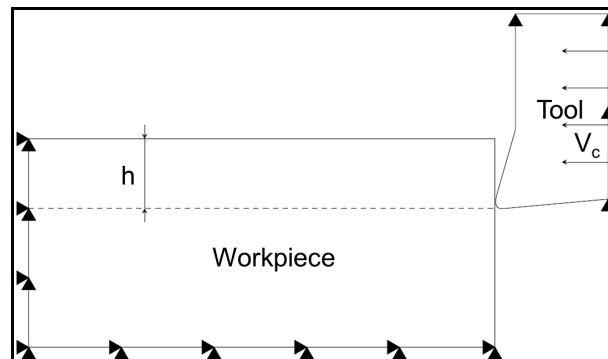


Fig. 2: Initial geometry and boundary conditions of the model.

The Hyperbolic TANgent (TANH) model introduced by Calamaz et al. [5] is used to describe the workpiece material behaviour. As shown on Fig. 3, the TANH law is a Johnson-Cook law modified in order to model the strain softening effect. It is observed in macro-cutting and could

explain the formation of saw-toothed Ti6Al4V chips. A more realistic chip should therefore be formed thanks to this law.

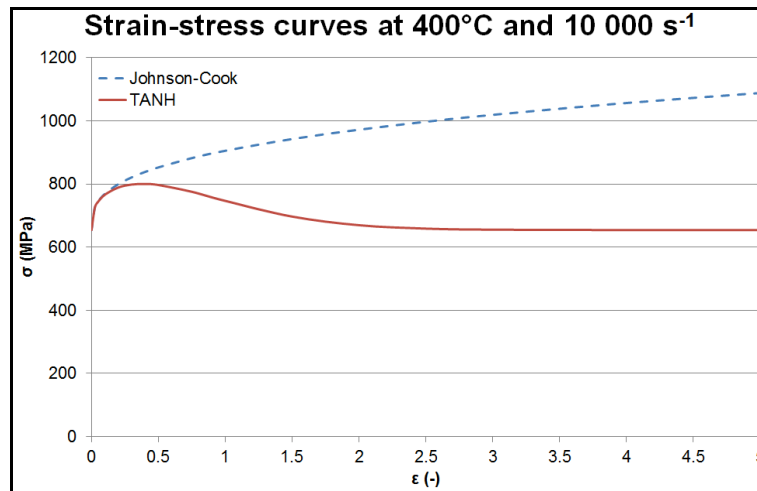


Fig. 3: Comparison between Johnson-Cook and TANH laws.

An explicit Lagrangian formulation is adopted as our interest is focused on the transient phase of the chip formation and the absence of chip generation. Moreover the model must be able to produce saw-toothed chips morphologically close to experimental ones, which cannot be achieved with an Arbitrary Lagrangian Eulerian (A.L.E.) formulation [6, 7], contrary to Lagrangian formulation [8].

Due to the Lagrangian formulation, a chip separation criterion based on an ‘eroding element’ method is introduced in the model to make chip formation possible. This separation criterion is based on the temperature dependent tensile failure of Ti6Al4V. As soon as the tensile failure value is reached in a finite element, it is deleted from the visualisation and all of its stress components are put to zero. The suppression of a finite element introduces a crack in the workpiece, making it possible for the chip to come off.

Coulomb’s friction is used to model friction at the tool – chip interface and all the friction energy is converted into heat, which is usually assumed [9]. The workpiece and tool initial temperature is set to 25°C. Only conduction is considered and all the parts faces are adiabatic.

The main input parameters of the model are synthetized in Table 1.

Macro-cutting results

In order to validate the model, the chip and the cutting forces are compared to experimental cutting results from literature [10] in the same conditions ($h = 280 \mu\text{m}$).

On Fig. 4a it can be seen that the morphology of the modelled chip is very close to the reference one, presented on Fig. 4b. Numerical teeth seem to be slightly deeper than experimental ones. For each tooth a slipping band is formed in the primary shear zone, as expected. It vanishes as the tool moves forward, initiating the tooth formation.

Fig. 5 shows the cyclic evolution of the cutting force (CF). Such a behaviour is typical of saw-toothed chip formation: a drop in the force happens during the formation of a tooth [13]. It can be seen on Fig. 4a and 5 that the number, 3, of teeth and drops is identical. It is also observed that the magnitude of the simulated force is of the same order of magnitude though slightly smaller than the reference one. The parameters choice of the TANH law [5] could explain this difference

Table 1: Main input parameters [5, 9-12, 14]

Parameter		Value	
Material	Behaviour	Ti6Al4V	TANH law
		Carbide	Linear elastic
	Density [kg/m ³]	Ti6Al4V	4430
		Carbide	15 000
	Young's modulus [GPa]	Ti6Al4V	113.8
		Carbide	800
	Poisson's ratio	Ti6Al4V	0.342
		Carbide	0.2
	Expansion [μm/m.K]	Ti6Al4V	4.7
		Carbide	4.7
	Conductivity [W/m.K]	Ti6Al4V	7.3
		Carbide	4.6
	Specific heat [J/kg/K]	Ti6Al4V	580
		Carbide	203
Inelastic heat fraction Ti6Al4V		0.9	
Friction energy to heat [%]		100	
Friction coefficient		0.05	

Process	Cutting speed [m/min]	75
	Depth of cut [μm]	280
	Tool edge radius [μm]	20
	Rake angle [°]	15
	Clearance angle [°]	2
	Width of cut [mm]	1
	Heat fraction to workpiece [%]	20

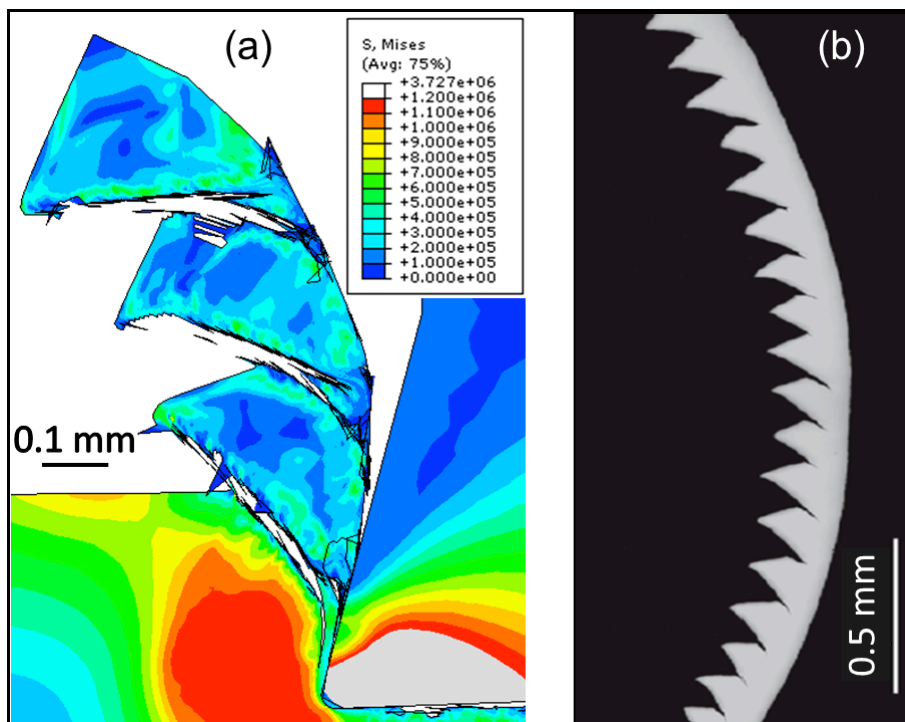


Fig. 4: (a) Von Mises stress contours (10^3 Pa) on modelled saw-toothed macro-chip, (b) Reference saw-toothed macro-chip [10].



Fig. 5: Macro-case cutting forces.

Similar observations are made on the feed force (FF) evolution: a link can be drawn between its cyclic evolution and the teeth formation (it can also be observed that when FF is maximal, CF is minimal, and vice-versa) and its magnitude is again of the same order of magnitude though slightly smaller than the reference force. That might be caused by the high influence of the friction at the tool – chip interface, which is difficult to measure and model

This model is thus able to reproduce the chip formation of Ti6Al4V in orthogonal cutting with a satisfactory fidelity. It is therefore appropriate to study the depth of cut influence on chip formation

Influence of the depth of cut

As for a determined material the minimum chip thickness depends on the depth of cut and the cutting edge radius of the tool, 8 decreasing values of the depth of cut have been considered (the cutting edge radius remaining constant, Table 1).

Table 2: Definition of the studied cases.

h [μm]	280	100	40	20	10	5	2.5	1
h/r	14	5	2	1	0.5	0.25	0.125	0.05

Chip morphology. Fig. 6 and 7 present the numerical chip morphologies obtained for the different depths of cut considered. It goes from saw-toothed chip to the absence of chip including segmented and nearly continuous chip. Under $h/r = 1$, the effective rake angle is negative and only the value of the cutting edge radius of the tool influences the chip formation.

The decrease of the depth of cut leads to a chip formation mechanism evolving away from macro-cutting: under $h/r = 0.25$ the material seems to be less sheared than pushed and deformed by the tool. This was also numerically noticed by Woon et al. [14]. According to them such a chip is formed by extrusion along the edge radius of the tool.

For h/r values from 0.125 no chip is formed and a small amount of material accumulates in front of the tool. This small amount grows when the tool moves forward until it reaches a thickness greater than the minimum chip thickness and is then removed from the workpiece. The fact that the chip is only formed when the accumulation of cutting thickness is higher than the minimum chip thickness has already been observed by Vogler et al. [15] for pearlite and ferrite.

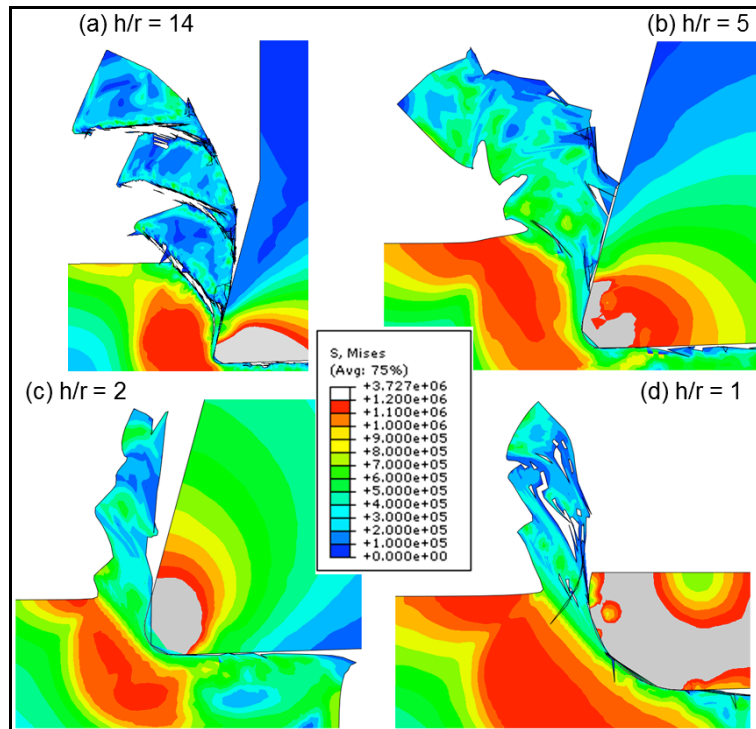


Fig. 6: Von Mises stress contours (10^3 Pa) during chip formation with $h/r = 14$ to $h/r = 1$.

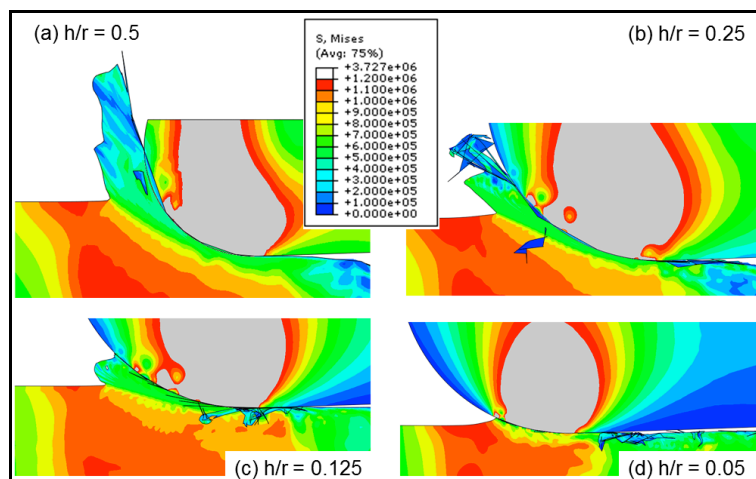


Fig. 7: Von Mises stress contours (10^3 Pa) during chip formation with $h/r = 0.5$ to $h/r = 0.05$.

When h/r decreases the primary shear zone fades and it cannot be distinguished any longer from the $h/r = 0.125$ value.

In the end, it can be concluded that changes in the chip formation mechanism happen for a value of the h/r ratio situated between 0.125 and 0.25.

Workpiece elastic spring back. During the cutting process, an elastic spring back (or elastic recovery) of the workpiece is observed after the tool tip passage. It has been estimated (by measuring the vertical distance between several points on the machined and the upper surface of the workpiece) for each simulated case in order to highlight its role in the cutting mechanism.

As shown on Fig. 8, a nonlinear increase of this elastic spring back is observed while the depth of cut decreases (from about 0.45% of h for 280 μm to about 25% of h for 1 μm). As its proportion, relatively to h , grows, it contributes to increase the feed force, the slipping forces and the specific cutting energy. This phenomenon is taking an increasing importance with the decrease of the depth of cut. The elastic spring back of the workpiece could be an indicator to evaluate the minimum chip

thickness. According to Fig. 8 the minimum chip thickness value is less than $10\ \mu\text{m}$: the elastic spring back evolution becomes exponential under this value.

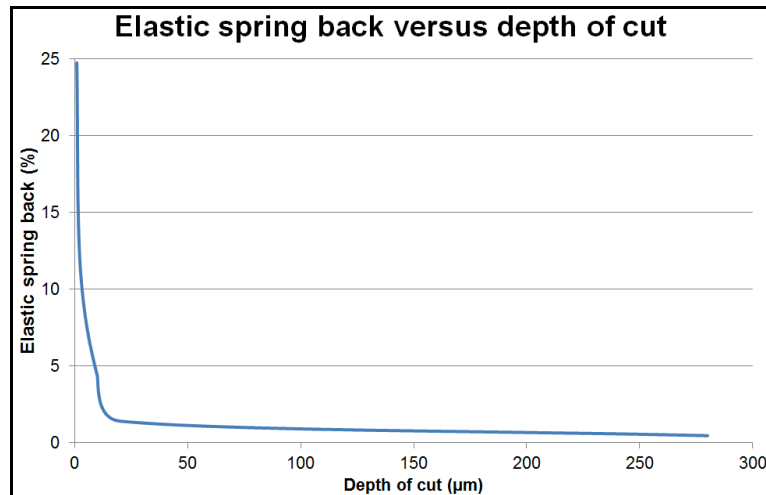


Fig. 8: Evolution of the workpiece elastic spring back with the depth of cut.

Cutting forces. When h/r decreases, the teeth are less marked and tend to disappear. The same observation is made for the cyclic forces evolutions. The feed to cutting forces ratio evolutions are presented on Fig. 9 for each value of the depth of cut. It can be seen that a decrease in the h/r ratio leads to an increase in the forces ratio. A change in the cutting mechanism is observed when the h/r ratio decreases: the feed force becomes greater than the cutting force (when the force ratio is greater than the unit), which has also experimentally been observed by Jun et al. [16]. This forces ratio can also be used to estimate the minimum chip thickness value. A critical value of the ratio sets to 2 (arbitrary chosen value greater than 1) leads to a minimum chip thickness value between $5\ \mu\text{m}$ and $10\ \mu\text{m}$.

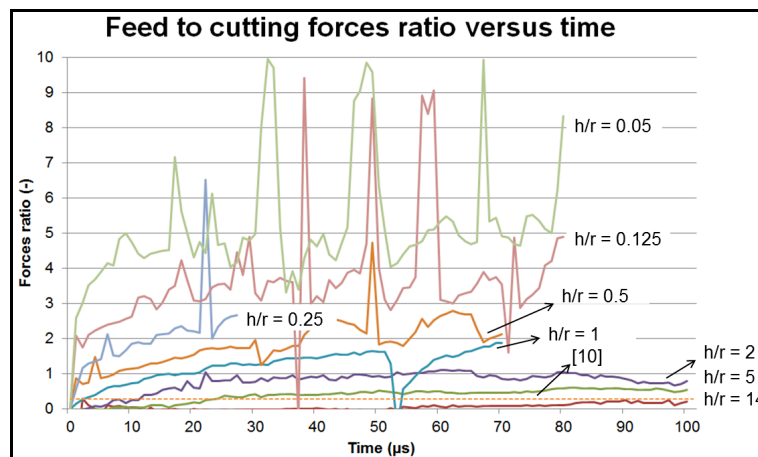


Fig. 9: Forces ratio evolutions for each depth of cut.

Specific cutting energy. Fig. 10 shows the mean normalized specific cutting energy versus depth of cut. This energy is the mean specific cutting energy from simulations divided by the reference cutting energy from Sun et al. [10] in order to get an adimensional quantity. This figure highlights the size effect: the specific cutting energy follows a nonlinear increase when the depth of cut decreases. Its evolution becomes exponential around $5\ \mu\text{m}$ - $10\ \mu\text{m}$. According to the size effect, the minimum chip thickness value is thus of the order of $5\ \mu\text{m}$ - $10\ \mu\text{m}$.

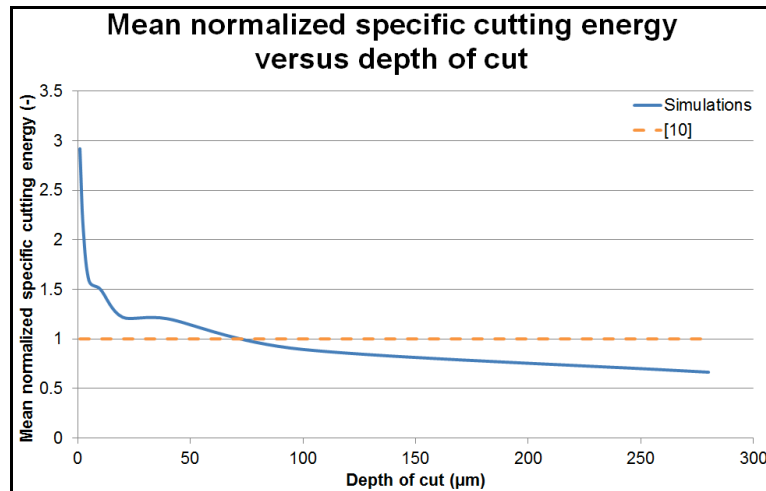


Fig. 10: Illustration of the size effect.

Minimum chip thickness prediction. For the geometry and the cutting condition of the model a minimum chip thickness prediction can be performed based on the previously presented results. It is obvious that the minimum chip thickness is less a precise and single value than a range of values with unclear limits. The elastic spring back of the workpiece sets the upper limit of the values range under 10 µm. The lower limit is set around 2.5 µm by the morphological aspect. The two others criterions, cutting forces and specific cutting energy, lead to a value between 5 µm and 10 µm.

The result of all the criterions is that the minimum chip thickness value is of the order of 5 µm (25% of r) with a lower limit around 2.5 µm (12.5% of r) and an upper limit inferior to 10 µm (50% of r). This order of magnitude is confirmed in literature [4, 17].

Conclusions

This paper highlights the changes in the cutting phenomenon induced by the transition from macro- to micro-cutting, from a geometrical point of view, through a 2D Lagrangian finite element model. These are the minimum chip thickness, the negative effective rake angle, the greater importance of the slipping forces and the scaling effect (already reported in literature). This work provides more details on the role and the importance of the elastic spring back of the workpiece and adds it to the micro-cutting features list. An estimation of the minimum chip thickness is also performed, leading to a value around 25% of the cutting edge radius of the tool.

References

- [1] Chae, J., Park, S., Freiheit, T.: *Int. J. Machine Tools and Manufacture*, 45 (2006), p. 313-332.
- [2] Weule, H., Hüntrup, V., Trischler, H.: *Annals of the CIRP*, 50 (2001), p. 61-64.
- [3] Simoneau, A., Ng, E., Elbestawi, M.A.: *Int. J. Machine Tools and Manufacture*, 46 (2006), p. 467-481.
- [4] Filiz, S., Conley, C., Wasserman, M., Ozdoganlar, O.: *Int. J. Machine Tools and Manufacture*, 47 (2007), p. 1088-1100.
- [5] Calamaz, M., Coupard, D., Girot, F.: *Int. J. Machine Tools and Manufacture*, 48 (2008), p. 275-288.
- [6] Ducobu, F., Filippi, E., Rivière-Lorphèvre, E.: *Proceedings of the 12th CIRP Conference on Modeling of Machining Operations*, (2009), p. 339-346.
- [7] Ducobu, F., Rivière-Lorphèvre, E., Filippi, E.: *Proceedings of the Eighth International Conference on High Speed Machining*, (2010), p. 202-207.

- [8] Ducobu, F., Filippi, E., Rivière-Lorphèvre, E.: Proceedings of the 9th International Conference on Laser Metrology, CMM and Machine Tool Performance, (2009), p. 327-336.
- [9] Nasr, M., Ng, E.G., Elbestawi, M., Proc. IMechE, Part B: J. Engineering Manufacture, 221 (2007), p. 1387-1400.
- [10] Sun, S., Brandt, M., Dargusch, M.S.: Int. J. Machine Tools and Manufacture, 49 (2009), p. 561-568.
- [11] Özel, T., Zeren, E.: Int. J. Machining and Machinability of Materials, 2 (2007), p. 451-468.
- [12] Lesuer, D.R., 2000, *Experimental investigations of Material Models for Ti-6Al-4V Titanium and 2024-T3 Aluminum*, Lawrence Livermore National Laboratory.
- [13] Bäker, M., Rösler, J., Siemers, C.: Comput. Struct., 80 (2002), p. 495-513.
- [14] Woon, K.S., Rahman, M., Fang, F.Z., Neo, K.S., Liu, K.: J. Materials Processing Technology, 167 (2007), p. 316-337.
- [15] Vogler, M.P., DeVor, R.E., Kapoor, S.G.: J. Manufacturing Science and Engineering, 126 (2004), p. 695-705.
- [16] Jun, M.B.G., DeVor, R.E., Kapoor, S.G.: ASME, 128 (2006), p. 901-912.
- [17] Vogler, M.P., DeVor, R.E., Kapoor, S.G.: J. Manufacturing Science and Engineering, 126 (2004), p. 685-694.